HHS Public Access

Author manuscript

Nat Microbiol. Author manuscript; available in PMC 2017 September 01.

Published in final edited form as:

Nat Microbiol. ; 2: 17020. doi:10.1038/nmicrobiol.2017.20.

A Mesh-Duox pathway regulates homeostasis in the insect gut

Xiaoping Xiao[1,2,3,4,#], **Lijuan Yang**[1,5,6,#], **Xiaojing Pang**[1,2,#], **Rudian Zhang**[1,5], **Yibin Zhu**[1,5], **Penghua Wang**[7], **Guanjun Gao**[1,5,*], and **Gong Cheng**[1,2,3,*]

[1]Tsinghua-Peking Center for Life Sciences, School of Medicine, Tsinghua University, Beijing, China, 100084

[2]Department of Basic Medical Sciences, School of Medicine, Tsinghua University, Beijing, P.R. China, 100084

[3]SZCDC-SUSTech Joint Key Laboratory for Tropical Diseases, Shenzhen Center for Disease Control and Prevention, Shenzhen, Guangdong, China, 518055

[4]Sino-French Hoffmann Institute, School of Basic Medical Science, Guangzhou Medical University, Guangzhou, P.R. China, 511436

[5]School of Life Science, Tsinghua University, Beijing, P.R. China, 100084

[6]College of Animal Science, Tarim University, Xinjiang, P.R. China, 843300

[7]Department of Microbiology and Immunology, School of Medicine, New York Medical College, Valhalla, NY, the United States, 10595

Summary

The metazoan gut harbors complex communities of commensal and symbiotic bacterial microbes. The quantity and quality of these microbes fluctuate dynamically in response to physiological changes. The mechanisms that hosts developed to respond to and manage such dynamic changes and maintain homeostasis remain largely unknown. Here, we identify a dual oxidase (Duox)-regulating pathway that contributes in maintaining homeostasis in the gut of both *Aedes aegypti* and *Drosophila melanogaster*. We show that a gut membrane-associated protein, named Mesh, plays an important role in controlling proliferation of gut bacteria by regulating *Duox* expression through an Arrestin-mediated MAPK JNK/ERK phosphorylation cascade. Expression of both *Mesh* and *Duox* is correlated with the gut bacterial microbiome that, in mosquitoes, increases

[*]Address correspondence to: Gong Cheng Ph.D., School of Medicine, Tsinghua University, Beijing, P.R. China, 100084. Phone: (+86)-10-62788494; Fax: (+86)-10-62788494; ongcheng@mail.tsinghua.edu.cn. Guanjun Gao Ph.D., School of Life Science, Tsinghua University, Beijing, P.R. China, 100084. Phone: (+86)-10-62772955; Fax: (+86)-10-62772955; gaogu@mail.tsinghua.edu.cn.

[#]These authors contributed equally to this work.

Correspondence and requests for materials should be addressed to G.C. (gongcheng@mail.tsinghua.edu.cn) and G.G. (gaogu@mail.tsinghua.edu.cn).

The authors declare that they have no competing financial interests.

Author Contributions

G.C. designed the experiments and wrote the manuscript; X.X. performed the majority of the experiments and analyzed data; X.P., R.Z. and Y.Z. helped with the RNA isolation and qPCR detection; L.Y. and G.G. provided the *Drosophila* systems and contributed in the investigations in *Drosophila*. P.W. contributed experimental suggestions and strengthened the writing of manuscript. All authors reviewed, critiqued and provided comments to the text.

dramatically soon after a blood meal. Ablation of *Mesh* abolishes *Duox* induction leading to an increase of the gut microbiome load. Our study reveals that the Mesh-mediated signaling pathway is a central homeostatic mechanism of the insect gut.

Introduction

The intestinal tract of most metazoans harbors complex communities of microbes that contribute to maintaining homeostasis with the gut epithelia. These microbes manipulate a wide range of physiological in the host, including nutrition, development, differentiation and defense[1–3]. Although these microbial communities maintain homeostasis with the gut epithelia, their quantity and composition dynamically fluctuate in response to the host dietary situations, environmental conditions and physical activities[4]. The gut epithelia have developed mechanisms to tolerate commensal microorganisms[5–10], while the microorganisms have developed mechanisms to evade the host immune response[11,12]. Nonetheless, the gut epithelia are required to mount a finely tuned immune response of proper strength and duration in response to microbial fluctuation in a timely and appropriate manner. The molecular mechanisms employed by the gut epithelia to manage the dynamic fluctuation of microbes and maintain homeostasis are not well understood.

Similar to the mammalian intestinal tract, the insect gut constantly interacts with its microbial residents. *Drosophila* and mosquitoes are established models for deciphering the complex interactions between the gut and its microbes[13,14]. Previous studies revealed that Dual oxidase (Duox)-mediated production of reactive oxygen species (ROS) is a major immune mechanism regulating insect gut-microbe homeostasis[6,7,15–17]. In *Drosophila*, Duox-mediated ROS are required for routine control of *Saccharomyces cerevisiae*, an essential microbial food source[6]. A reduction in ROS levels in the midgut of the major arboviral vector mosquito *Aedes aegypti* results in dysbiotic proliferation of the intestinal microbiota[15]. Duox-mediated ROS also play a pivotal role in regulating homeostasis and the composition of the gut bacterial community in *Bactrocera dorsalis*[16] and *Phlebotomine* sandflies[17]. Indeed, under homeostatic conditions, both the expression and activity of Duox are tightly restricted to a level that allows healthy gut-microbe interactions, thereby precluding any pathophysiological effects on the gut epithelia. Induction of *Duox* gene expression is limited in an off-state status by phospholipase Cβ (PLCβ)-mediated mitogen-activated protein kinase (MAPK) P38 dephosphorylation in the *Drosophila* gut epithelia[7]. Modest ROS levels are achieved by activation of basal Duox expression through intracellular Ca^{2+} mobilization by a G-protein α subunit q protein (Gαq)-PLCβ signal cascade[6,18]. Thus, the basal expression and activation of Duox are essential to manage symbiotic microbes under healthy conditions in the insect gut.

The complement control protein (CCP) domain is an evolutionarily conserved module essential for complement-mediated immune functions[19–22]. We have previously demonstrated that the CCP domain plays an important role in insect-microbe interactions[23,24]. In this study, we show that a CCP-containing protein named Mesh[25] regulates commensal bacterial proliferation through regulation of *Duox* expression in the gut of both *Drosophila* and *A. aegypti*, via a signaling cascade involving Arrestin-mediated

MAPK JNK/ERK phosphorylation. In both insects, *Mesh* expression correlates with the gut commensal bacterial load, enabling *Duox* abundance to be dynamically regulated by microbial fluctuation. Since generation of Duox-mediated ROS is a major gut immune response in maintenance of insect gut homeostasis, our study reveals a fine-tuning mechanism for *Duox* expression to manage healthy gut-microbe interactions in insects.

Results

Mesh controls *Duox* expression and gut microbiome load in *A. aegypti* and *Drosophila*

Proteins with CCP domains are key immune factors restricting microbial infection in invertebrates[23,24,26]. Here, we assessed the roles of CCP-domain proteins[23] in maintenance of the gut commensal bacteria in the mosquito *A. aegypti*. Ten genes encoding CCP domains[23] were silenced individually via thoracic microinjection of double-stranded RNA (dsRNA). Six days later, the midguts of dsRNA-treated mosquitoes were dissected for determination of the gut bacterial load by qPCR[27]. The results showed that knockdown of the *AAEL005432* gene, but not other genes, significantly induced 4- to 5-fold proliferation of the gut microbiome in *A. aegypti*, compared to that found in *green fluorescent protein* (*GFP*) dsRNA-treated *A. aegypti*, suggesting an antibacterial role of this protein in mosquito gut immunity (Fig. 1a). *AAEL005432* shares high sequence identity with the *Drosophila melanogaster Mesh* (*CG31004*) (*DmMesh*) that was previously identified as a transmembrane component of the gut septate junctions[25] (Supplementary Fig. 1a). Moreover, the *AAEL005432*-encoded protein is predicted to contain domains that are identical to those of DmMesh (Supplementary Fig. 1b). Therefore, we refer to this gene as *A. aegypti Mesh*, i.e. *AaMesh*.

We assessed *AaMesh* expression in various tissues of *A. aegypti* by qPCR. We noted that *AaMesh* abundance varied among mosquito tissues. The *AaMesh* transcript in the midgut is 6- to 11-fold higher than that in the Malpighian tubules and salivary glands, and more than 20- fold higher than that in head, hemolymph and ovaries (Supplementary Fig. 2a), which is consistent to the previous reports[28,29]. Therefore, we speculated that *AaMesh* expression levels might coincide with the gut bacterial loads. Indeed, oral feeding of mosquitoes with antibiotics repressed *AaMesh* expression in the midgut (Supplementary Fig. 2b). Conversely, *AaMesh* expression in the gut was gradually induced after a blood meal over a time course (Supplementary Fig. 2c), most likely as a result of microbial proliferation[15,27].

To validate the role of AaMesh in controlling the gut microbiome, we expressed and purified an AaMesh peptide (994 aa-1174 aa) from *Escherichia coli* cells (Supplementary Fig. 3a) and generated a mouse polyclonal antiserum against this fragment (Supplementary Fig. 3b). The antiserum recognized a protein band corresponding to AaMesh in control mosquito lysates, which was impaired from the *AaMesh*-silenced mosquitoes demonstrating the specificity of the antiserum (Fig. 1b). We added the antiserum into the *A. aegypti* blood meal and measured the gut microbiome load 12 and 24 hours later. The result showed that immuno-blockade of AaMesh significantly increased the gut microbiome load at both time points (Fig. 1c).

To investigate the molecular mechanism by which Mesh restricts the gut microbiome proliferation, we collected midguts from *AaMesh* dsRNA-inoculated (Day 3 and 6) and AaMesh antiserum-fed (18 hours) mosquitoes, respectively. Midguts of *GFP* dsRNA-treated and pre-immune antiserum-fed mosquitoes served as controls. RNA-Seq and in-depth analysis of immune-related genes identified 48 genes in anti-AaMesh antiserum-treated guts, and 44 genes in 3 day- and 52 genes in the 6 day-*AaMesh* dsRNA-treated guts as significantly downregulated compared to their respective controls (Supplementary Fig. 4a,b and Supplementary Table 1). Five of these genes were detected in all three experimental groups, including *A. aegypti Arrestin a* and *b* (*AaArrestin*), *Duox* (*AaDuox*), *haemopexin 7* (*AaHPX7*) and *C-type lysozyme 9* (*AaLYSC9*) (Supplementary Fig. 4c). Of these, Duox is a member of the ROS-generating nicotinamide adenine dinucleotide phosphate (NADPH) oxidases. Generation of Duox-mediated ROS is a major immune mechanism regulating gut-microbe homeostasis in insects[6,7].

We validated the regulation of *AaDuox* (*A. aegypti Duox*) in the gut of *AaMesh*-silenced mosquitoes by qPCR. The mRNA abundance of *AaDuox* was significantly downregulated 4–6 folds at 3 and 6 days post *AaMesh* silencing, compared to the *GFP* dsRNA-treated controls (Fig. 1d). In consistence with this finding, ROS activity measured by H_2O_2 assay (Fig. 1e) and Dihydroethidium (DHE) staining (Fig. 1f) was consistently suppressed in the gut of *AaMesh*-silenced mosquitoes. We also measured ROS activity after feeding mosquitoes with AaMesh antiserum through the blood meal. The results showed that immuno-blockade of AaMesh dramatically impairs the *AaDuox* expression (Fig. 1g) and ROS activity (Fig. 1h), respectively.

Next, we assessed the conservation of the role of Mesh in controlling the gut microbiome by regulating *Duox* expression in the model insect *D. melanogaster*. *DmMesh* is previously shown to be an essential component of gut development[25]. We exploited a *UAS/GAL4* system to knock down *DmMesh* expression specifically in the *Drosophila* midgut, via a specific *GAL4* line driven by a midgut-specific *NP3084* promoter. Since Mesh was known to involve in the formation of septate junction[25], we therefore tested the gut integrity of the *DmMesh* RNAi flies, via a Smurf assay[30]. Silencing *DmMesh* does not impair the gut integrity (Supplementary Fig. 5). Compared to the *GFP-RNAi* control flies, both *DmMesh* mRNA and protein levels were consistently impaired in the gut of *DmMesh* RNAi flies (Fig. 2a,b). We next examined the role of *DmMesh* in regulating the expression of *DmDuox* (*CG3131*). *DmDuox* expression (Fig. 2c) and ROS activity (Fig. 2d) were much lower in the guts of *DmMesh* RNAi flies respectively. Consistently, the *DmDuox* mRNA levels were significantly reduced in early-stage 1st instar *DmMesh*$^{-/-}$ compared to wild-type larvae (Supplementary Fig. 6a,b). To further assess the regulation of *DmDuox* by DmMesh, we cloned *DmMesh* into a pAc5.1/V5-His expression vector (pAc-DmMesh). Ectopic expression of DmMesh in *Drosophila* S2 cells resulted in more than 3-fold higher expression of the *DmDuox* (Supplementary Fig. 7). In accordance to the observation in *A. aegypti*, the gut microbiome load was significantly increased by ~3-fold in *DmMesh* RNAi *Drosophila* compared to *GFP* RNAi controls (Fig. 2e), confirming a key role of Mesh in restricting the proliferation of the gut microbiome in insects. We next rescued the *DmDuox* into *DmMesh*-RNAi flies to test whether over-expression of *DmDuox* can rescue the effects on bacterial

burden. The gut bacterial burden was significantly reduced in the *DmDuox*-rescued *DmMesh*-RNAi *Drosophila*, compared to that in the gut of *DmMesh* RNAi flies (Fig. 2f).

We next determined whether the Mesh-Duox signaling axis changes the gut microbial composition in *Drosophila* and *A. aegypti*. The midguts were isolated from the mosquitoes (*AaMesh* dsRNA vs *GFP* dsRNA) and *Drosophila* (*DmMesh* RNAi vs *GFP* RNAi) for bacterial 16S rDNA pyrosequencing. Intriguingly, dsRNA-mediated *AaMesh* knockdown enhanced the composition of *Firmicutes* and *Proteobacteria*, but decreased that of *Actinobacteria* and *Bacteroidetes* in the midgut of *A. aegypti* (Supplementary Fig. 8a,b and Supplementary Table 2,3). In *Drosophila*, enhancement of *Proteobacteria* and impairment of *Bacteroidetes* and *Firmicutes* in bacterial composition were determined in the gut of *DmMesh* RNAi flies (Supplementary Fig. 8c,d and Supplementary Table 4,5), suggesting that the Mesh-Duox axis-based regulation pathway is specific for particular bacterium.

Mesh regulates *Duox*, but not *Nox* expression, for ROS production

In insect intestine, ROS is produced via the catalytic action of NADPH oxidases, including Nox[31] and Duox[7,32]. A particular commensal bacteria genus in the *Drosophila* guts, *Lactobacillus*, can stimulate Nox-dependent ROS production to facilitate cellular proliferation in intestinal stem cells. A specific Nox-dependent ROS generation in the gut epithelial cells may act as an important role in ROS-mediated intestinal homeostasis[33]. Nevertheless, many previous studies indicated the pivotal roles of Duox in regulating homeostasis and the composition of the gut commensal bacterial community in *Drosophila*[6], *Aedes aegypti*[15] and *Bactrocera dorsalis*[16]. To address this, we therefore generated both *DmNox* (*CG34399*) RNAi and *DmDuox* RNAi *GAL4 Drosophila* lines driven by a midgut-specific *NP3084* promoter. Compared to that in the *GFP* RNAi control flies, the burden of gut commensal bacteria was enhanced in both the *DmNox* RNAi and the *DmDuox* RNAi *Drosophila* gut (Supplementary Fig. 9a,b). We further silenced either *A. aegypti Nox* (*AaNox*) or *AaDuox* by dsRNA inoculation in *A. aegypti*, respectively. In consistent with the studies in flies, knockdown of both *NADPH oxidase* genes also enhanced the burden of gut microbiota in the mosquito midgut (Supplementary Fig. 9c,d), suggesting both NADPH oxidases are important for the ROS-mediated intestinal homeostasis.

We next explored *Nox* regulation in the Mesh-mediated signaling pathway. In contrast to the significant *DmDuox* reduction in the *DmMesh* RNAi fly guts, expression of the *DmNox* gene was not regulated by silencing *DmMesh* (Supplementary Fig. 9e). Furthermore, there was no influence of *AaNox* transcript in the gut of dsRNA-mediated *AaMesh*-silenced mosquitoes (Supplementary Fig. 9f), suggesting that Mesh controls insect gut-microbe homeostasis by regulating the expression of *Duox*, but not *Nox* gene.

Mesh regulates *Duox* expression via Arrestin-mediated MAPK phosphorylation

We examined the roles of major immune signaling pathways in *AaDuox* and *AaMesh* expression in the mosquito gut through dsRNA-mediated knockdown of key pathway modulators, including components of the MAPK pathways (*AaP38*, *AaERK* and *AaJNK*), *AaMyd88* of the Toll pathway, *AaImd* of the Immune deficiency (Imd) pathway, *AaDome* of (Janus kinase (JAK)-signal transduction and activators of transcription (STAT) pathway),

phosphatidylinositol 3-kinase (*AaPI3K*) and *AaAkt* of the PI3K-AKT-mTOR pathway (Supplementary Fig. 10a–h). Silencing either *AaERK* or *AaJNK*, but not any of the other immune signaling modulators, significantly reduced *AaDuox* expression in the mosquito midgut (Fig. 3a). However, none of the above-mentioned gene knockdowns affected *AaMesh* mRNA levels (Supplementary Fig. 10i), suggesting that *AaERK* and *AaJNK* may act downstream of *AaMesh*, but upstream of *AaDuox*. Indeed, knockdown of either *AaERK* or *AaJNK* reduced ROS production in the *A. aegypti* gut (Supplementary Fig. 11a,b), and increased the gut microbiome load (Fig. 3b,c).

Besides *AaDuox*, the expression levels of two *A. aegypti Arrestin* genes (*AaArrestin-a* and *AaArrestin-b*) were also downregulated in both anti-AaMesh antiserum-treated and *AaMesh* dsRNA-treated guts (Supplementary Fig. 4c and Supplementary Fig. 12a,b). In mammals, β-arrestin, the orthologue of insect Arrestins, is essential for the MAPK signaling cascade by forming a transduction scaffold for phosphorylation of MAP kinases, especially ERK and JNK[33]. Therefore, we assessed the role of *AaArrestins* in the "MAPK-Duox" cascades. Genetic suppression of either *AaMesh* or *AaArrestins* expression (Supplementary Fig. 12c,d) impaired the phosphorylation of both AaERK and AaJNK MAPK kinases in the mosquito gut (Fig. 3d). Knockdown of *AaMesh* did not significantly affect the expression of *AaERK* and *AaJNK* (Supplementary Fig. 13a,b). In addition, both the *AaDuox* expression (Fig. 3e) and ROS activity (Fig. 3f) were consistently reduced in the *AaArrestins*-silenced guts, resulting in expansion of the gut microbiome 3 and 6 days after *AaArrestins* knockdown (Fig. 3g). These data suggested that a Mesh-Arrestin-ERK/JNK signaling cascade might control Mesh-mediated *Duox* expression.

We next tested our findings in the *Drosophila* gut by exploiting the *UAS/GAL4* system to knockdown *DmERK* (*CG12559*) and *DmJNK* (*CG5680*) via *GAL4* lines driven by the *NP3084* promoter. Both *MAPK* genes were stably knocked down in the *Drosophila* gut (Supplementary Fig. 14a,b), resulting in a significant downregulation of *DmDuox* expression (Fig. 4a,b), a reduction of ROS activity (Fig. 4c) and an increase of the gut bacterial load (Fig. 4d). We next exploited *DmArrestin-1* (*CG5711*) and *DmArrestin*-2 (*CG5962*) RNAi flies for investigation. Silencing *DmArrestin-1* and *DmArrestin-2* showed the consistent phenotypes in regulation of *DmDuox* expression (Fig. 4e), ROS activity (Fig. 4f) and gut bacterial burden (Fig. 4g). To further examine the role of the Mesh-Arrestin-ERK/JNK signaling cascade in *Duox* expression, we silenced both of the *DmArrestin* genes by dsRNA transfection in *Drosophila* S2 cells (Supplementary Fig. 15a,b) that ectopically express DmMesh, and then examined the *DmDuox* mRNA abundance. Indeed, ectopic expression of *DmMesh* induced ERK/JNK phosphorylation (Fig. 4h) and *Duox* expression (Fig. 4i), which were abolished following knockdown of either of the *DmArrestins*, further validating that Mesh regulates *Duox* expression via Arrestin-mediated MAPK phosphorylation. We next introduced the *DmDuox* gene into *DmArrestins* RNAi flies respectively to test whether *DmDuox* over-expression can rescue the effects on gut bacterial burden. The gut bacterial burden was significantly decreased in the *DmDuox*-rescued *DmArrestin*-RNAi *Drosophila*, compared to that in the gut of *DmArrestin* RNAi flies (Supplementary Fig. 16a,b).

Mesh-mediated *Duox* expression correlates with the gut commensal bacterial load

In hematophagous insects such as mosquitoes, gut commensal bacteria proliferate rapidly during blood meal digestion. We investigated the correlation between the Mesh-mediated *Duox* expression and the microbiome load in the *Aedes* gut following a blood meal. The gut microbiome load increased drastically reaching a peak at about 30 hours post blood feeding (Fig. 5a). The expression levels of *AaMesh*, *AaArrestins* and *AaDuox* were also significantly and progressively upregulated after blood feeding, coinciding with the microbiome expansion (Fig. 5b–e). Silencing *AaMesh* completely abolished the induction of *AaDuox* expression after a blood meal (Fig. 5f).

We examined whether the upregulation of *AaMesh*, *AaArrestins* and *AaDuox* observed after blood feeding can be correlated with specific members of the mosquito gut microbiome. Both *Comamonas testosteroni* and *Chryseobacterium meningosepticum* have been routinely identified as cultivable gut commensals in *Aedes* mosquitoes[12,34]. These 2 bacteria robustly proliferated in response to a blood meal and by suppressing the Mesh-mediated signaling (Supplementary Fig. 17). We next cultured these bacteria[12] and orally fed these bacteria to antibiotic-treated mosquitoes through the blood meal (Supplementary Fig. 18a,b). The *AaMesh*, *AaArrestins* and *AaDuox* genes were upregulated by oral introduction of *C. testosteroni* (Fig. 5g–j) and *C. meningosepticum* (Fig. 5k–n) in a dose-dependent manner. These findings were also tested in *Drosophila*. We identified *Acetobacter thailandicus* as a cultivable bacterium from the *Drosophila* gut[35]. Moreover, composition of *A. thailandicus* was dramatically regulated in the gut of *DmMesh* RNAi flies (Supplementary Fig. 8d). Oral introduction of serial quantities of *A. thailandicus* cells (Supplementary Fig. 18c) in the germ-free fly guts (Supplementary Fig. 19) induced the expression of *DmMesh* in both mRNA transcript (Fig. 6a) and protein (Fig. 6b) levels. In consistent, the *DmDuox* expression (Fig. 6c) and ROS activity (Fig. 6d) were dramatically induced by the bacterial oral introduction in a dose-dependent manner. Both *DmDuox* induction (Fig. 6e) and the ROS enhancement (Fig. 6f) were abolished in *DmMesh* RNAi flies.

In addition to commensal gut bacteria, the gut epithelia may be also face infected by pathogenic bacteria. We next determined the role of Mesh-Duox axis in response to pathogen infection. A *Drosophila* pathogen, *Erwinia carotovora carotovora 15* (*Ecc15*), was fed to both *DmMesh* RNAi and control flies. Since *Ecc15* can trigger a strong systemic immune response following oral infection[32], the *DmDuox* gene was dramatically up-regulated in the midgut of both *DmMesh* RNAi and control flies (Supplementary Fig. 20). These data suggest that the Mesh-Duox axis may only play a fine-tuning role in conventional condition (Fig. 6g).

Discussion

The quantity and quality of the gut symbiotic bacteria fluctuate dynamically with gut activities such as alimentary flow, food ingestion and other physiological changes[36]. The host senses these changes and fine-tunes its gut immune system to respond with proper strength and duration to the dynamic changes in commensal microbes. In mammals, ROS plays an important role in controlling the normal gut microbiota. The previous studies indicated that Duox2, an important source of hydrogen peroxide, can be induced by normal

gut microbiota in mice[37]. In addition to Duox2-induced ROS generation, NADPH oxidase 1 (Nox1) also acts as a key player for ROS responses in the murine intestine, particularly induced by members of the genus *Lactobacillus*[31], revealing an important role of commensal bacteria-mediated ROS generation in maintenance of homeostasis in the mammalian intestine.

It is largely unknown how the insect gut epithelium might sense the dynamic changes of the microbiome and adjust its response. Several studies in *Drosophila* and other insects have revealed that the gut epithelia rely on basal production of Duox-dependent ROS for maintaining gut-microbe homeostasis[16,17,38]. Here, we identified Mesh as an indispensable factor of the *A. aegypti* and *D. melanogaster* gut, which fine-tunes the expression of *Duox* and production of ROS, thereby regulating the gut bacterial load. The expression level of *Mesh* correlates with the load of gut bacteria, which in mosquitoes are induced dramatically after a blood meal. Mechanistic studies have demonstrated that Mesh mediates constitutive *Duox* expression in the gut via an Arrestin-MAP kinase signaling cascade. First, silencing *Mesh* abolishes bacterially induced *Duox* expression, while its ectopic overexpression increases *Duox* levels. Second, depletion of the gut microbiome reduces *Mesh* expression, while reconstitution of the microbiome recovers *Mesh* and *Duox* expression level in a microbial burden-dependent manner. Third, silencing either of the *Arrestins*, *JNK* or *ERK* abolishes Mesh-mediated *Duox* expression. Taken together, these results suggest that Mesh, directly or indirectly, senses the dynamic fluctuation of the gut microbiome thereby transmitting a signal to an intracellular signaling cascade to fine-tune the antibacterial immune responses and restore homeostasis.

Mesh has a complement control protein (CCP) domain, which is an evolutionarily conserved immune module that recognizes microbial ligands. Scavenger Receptor-C (SR-C), a *Drosophila* membrane receptor that also contains 2 CCP domains, is capable of recognizing both Gram-positive and Gram-negative bacteria acting as a pattern recognition receptor for phagocytosis in hemocytes[26]. Moreover, the CCP module of various *A. aegypti* immune factors mediates direct recognition of Dengue viral particles restricting viral infection[23,24]. Our preliminary data suggest that neither of *Aedes* or *Drosophila* Mesh (expressed as full-length proteins in *Drosophila* S2 cells) can directly interact with *C. testosteroni*, *C. meningosepticum* or *A. thailandicus*, which are common members of the insect microbiome. In addition to surface bacterial components, metabolites generated by gut microbes can also contribute to the regulation of gut immunity. It is known that bacterial-derived uracil acts as a modulator to boost the ROS activity in *Drosophila*[38]. Future work should aim to investigate bacterial ligands for the Mesh-mediated *Duox* expression.

RNA-Seq and in-depth analysis of immune-related genes identified that 5 genes were consistently down-regulated in both *AaMesh*-silenced and AaMesh-immuno-blockaded mosquito guts. In these 5 genes, LYSC9 is an enzyme with bactericidal activity[39,40]. Duox is a member of the ROS-generating NADPH oxidases. Besides the *Duox* gene that we focused on this study, expression of a *C-type lysozyme 9* (*LYSC9*) was also significantly impaired by immuno-blocking/silencing AaMesh, suggesting expression of LYSC9 might be controlled by Mesh-mediated signaling. Recent studies showed that a *C. elegans* lysozyme, known as invertebrate-type lysozyme-3 (ilys-3), can be up-regulated by ERK-MAPK-

dependent signaling in the worm intestine, during challenge with Gram-positive pathogens[41]. Indeed, our studies have demonstrated that Mesh mediates down-stream gene (*Duox*) expression via the ERK/JNK MAPK signaling cascade. We therefore speculate that LYSC9 might also be counted as one of the Mesh-mediated MAPK signaling-regulated genes, and contribute to fine-tuning the gut-microbe homeostasis in insects. The role of LYSC9 in the regulation of microbiota will be investigated in our further study.

In addition to commensal gut bacteria in *Drosophila* and mosquitoes, the gut epithelia also face invasion from allochthonous microorganisms with pathogenic properties. The proliferation of these pathogens and their metabolites stimulates the epithelia to generate ROS at a much higher level than under conventional conditions[7,38]. Induction of the *Duox* in the *Drosophila* gut is mediated by the MAP kinase kinase kinase (MEKK1)-MAP kinase kinase 3 (MKK3)-P38-ATF2 pathway. Gαq-mediated PLC-β directly activates MEKK1, thereby leading to the MAPK P38-dependent *Duox* induction[7]. However, under healthy conditions, the expression of *Duox* is off-set by MAPK P38 dephosphorylation via PLC-β-MAP kinase phosphatase-3 (MKP3) signaling[7], indicating that the MAPK P38 signaling cascade plays a central role in regulating *Duox* expression during pathogenic microbial infections. Moreover, MAPK P38 pathway deficient flies can survive with conventional rearing, suggesting that the MAPK P38-mediated cascade is dispensable for the maintenance of basal *Duox* expression in healthy gut-microbe interactions[7,18]. Here, we show that indeed Mesh constitutively regulates the basal *Duox* expression via phosphorylation of the MAP kinases JNK and ERK but not P38. We also show that these phosphorylation events are mediated by Arrestins, the expression of which is also controlled by the pathway. Indeed, previous studies have shown that the mammalian β-arrestin acts as a signal transduction scaffold for MAP kinases, and is thereby essential for the MAPK signaling cascade[33].

The current findings suggest that Mesh-mediated *Duox* induction is a bacterium-specific response. However, three important questions remain unanswered: 1) is this pathway responsive to all the commensal bacteria or specific classes? 2) how does Mesh sense bacteria, the bacterial surface PAMPs or secreted metabolites? and 3) is this pathway applicable to the mammalian system? Addressing these questions in our future endeavors may not only provide a complete picture of delicate interactions between microbiota and host, but also a conceptual advancement in general.

Methods

Mosquitoes, *Drosophila* and bacteria

Aedes aegypti (the Rockefeller strain) was maintained in the laboratory in a low-temperature illuminated incubator (model 818, Thermo Electron Corporation, Waltham, MA, USA) at 26°C and 80% humidity according to standard rearing procedures[23,42]. The 5-day old female mosquitoes were used for the experiment. *D. melanogaster* were maintained on standard cornmeal-agar medium at 25°C in 60% relative humidity. *Drosophila* S2 cells were cultured at 28°C in Schneider's *Drosophil*a medium, which was supplemented with 10% heat-inactivated fetal bovine serum, 1% L-glutamine, and 100 U/ml each of penicillin and streptomycin. Both *C. testosteroni* and *C. meningosepticum* from the midguts of *A. aegypti*,

and *A. thailandicus* from the midguts of *D. melanogaster* were isolated, and subsequently cultured on LB plates without any antibiotics at 37°C.

Antibody

A fragment of the *AaMesh* gene (2980 bp-3522 bp) was amplified from *A. aegypti* cDNA and cloned into a pET-28a (+) expression vector. The cloning primers are presented in Supplementary Table 6. The recombinant peptide was expressed in the *E. coli* BL21 DE3 strain, with the insoluble form in inclusion bodies. The proteins were resolved with 8 M urea and purified using a purification kit (Clontech, Cat. No# 635515). Polyclonal antibodies were produced by 3 boosting immunizations in C57BL/6 mice. The antibodies for the phosphorylated DmERK and DmJNK were purchased from Sigma Aldrich (Cat. No# M9692) and Thermo Fisher (Cat. No# MA5-14943), respectively. These antibodies for DmERK and DmJNK can efficiently detect the phosphorylated AaERK and AaJNK in *A. aegypti*. The antibodies for the tags were purchased from the Medical & Biological Lab (MBL, Japan).

Genetic manipulation in the *Drosophila* S2 cells

DmMesh was amplified from the *Drosophila* cDNA library and then cloned into the pAc5.1-V5/His A vector (Invitrogen, Cat. No# V4110-20). The *GFP* gene was cloned into the same plasmid as a mock control. The recombinant plasmids were designated pAc-DmMesh and pAc-GFP, respectively. For gene silencing study, the dsRNA was synthesized as previously described[43]. The S2 cells were seeded at 2×10^6 cells/mL per well in a 6-well plate. Then, dsRNA or recombinant plasmids were premixed with Effectene® (Qiagen, Cat. No# 301425), according to the manufacturer's instructions, and consequently used for transfection.

Silencing genes in the *A. aegypti* mosquitoes

The synthesis of dsRNA was performed as previously described[43]. The primers are shown in Supplementary Table 6. We described the detailed procedures used for gene silencing in mosquitoes elsewhere[23,42,43]. Briefly, the mosquitoes were cold-anesthetized on a cold tray (BioQuip, USA), and 1 μg/300 nl of dsRNA was subsequently microinjected into the mosquito thoraxes. The injected mosquitoes were allowed to recover under standard rearing conditions and were used for the subsequent investigations.

Generation of the homozygous *DmMesh*$^{-/-}$ flies

Using a two-component CRISPR/Cas9-mediated gene targeting system[44], a *Mesh* mutation line with mutations and deletions was generated via the non-homologous end joining (NHEJ) pathway. Briefly, we co-injected Cas9-mRNA and *Mesh*-specific gRNAs into w1118 early embryos. The recovered male F_0 flies were then crossed to w; *atm/TM6B.Act5c-GFP* flies to obtain the F_1 progeny with germline-transmitted mutations. It was balanced with a GFP-expressing *Tm6B* balancer to distinguish homozygous *DmMesh*$^{-/-}$ flies from heterozygous flies. The mutation in the *Mesh* locus was consequentially verified by PCR and DNA sequencing[45]. Primers used for gRNA, PCR and sequencing are listed in Supplementary Table 6.

RNAi *Drosophila* strains

Drosophila DmMesh RNAi (VDRC, Cat. No# 108297), *DmArrestin-1* RNAi (VDRC, Cat. No# 109860), and *DmArrestin-2* RNAi (VDRC, Cat. No# 20989) lines were provided by the Vienna *Drosophila* RNAi Center. *DmERK* RNAi (THFC, Cat. No# THU5780), *DmJNK* RNAi (THFC, Cat. No# THU1781), *DmDuox* RNAi (THFC, Cat. No# THU1093), *DmNox* RNAi (THFC, Cat. No# THU0880) and *Ubi-GAL4* (THFC, Cat. No# TB00152) were obtained from the Tsinghua Fly Center (THFC, Beijing, China). *UAS-GFP* RNAi (VDRC, Cat. No# 41557) was purchased from the Bloomington *Drosophila* Stock Center (Bloomington, IN, USA) and *NP3084* (DGRC, Cat. No# 113094) was purchased from the KYOTO Stock Center (DGRC) (KYOTO, Japan).

Rescuing *DmDuox* into *DmMesh* RNAi and *DmArrestins* RNAi *Drosophila* strain

The entire open reading frame of the *DmDuox*-cDNA were subcloned into the pWALIUM20 vector[46] to obtain the *UAS-DmDuox*-cDNA construct, respectively. These constructs were then used to generate transgenic rescue flies through the φC31-mediated recombination between *attB* and the corresponding pseudo *attP* sites. The *UAS-DmDuox*-cDNA was built on the second chromosome. The transgenic flies (*UAS-DmDuox*-cDNA) were used to rescue the phenotypic defects of *DmMesh* RNAi, *DmArrestin-1* RNAi and *DmArrestin-2* RNAi flies, respectively. In briefly, the transgenic flies with DmDuox over-expression (*UAS-DmDuox*-cDNA strain) were used to crossed with *UAS-DmMesh*-RNAi flies to obtain the final strains carrying one copy of the *UAS-DmMesh*-RNAi construct with one copy of the *UAS-DmDuox*-cDNA. As well, we obtained the final strains carrying one copy of either *DmArrestin-1* RNAi or *DmArrestin-2* RNAi construct with one copy of the *UAS-DmDuox*-cDNA flies.

Generation of germ-free *Drosophila* and bacterial oral feeding

To generate germ-free flies, eggs were washed in sterile deionized water, immersed in 2.7% sodium hypochlorite solution for 2 minutes. Embryos were subsequently washed twice in 70% ethanol, followed by three washes with sterile water. Embryos were transferred to axenic standard fly food vials for rearing. The bacteria cells, which were collected in exponential growth phase, were mixed with the standard *Drosophila* food to feed the germ-free flies.

Antibiotic treatment mosquito and bacterial oral feeding

Mosquitoes were treated using cotton balls moistened with a 10% sucrose solution including 20 units of penicillin and 20 μg of streptomycin per milliliter for 3 days[47,48]. Then, the mosquitoes were starved for 24 hours to allow the antibiotics metabolized prior to bacterial challenge. The mosquitoes were decontaminated in 70% ethanol and rinsed in sterile PBS, and the midguts were dissected under aseptic conditions. The removal of the microbes was confirmed by qPCR using a universal bacteria primer[27] and a colony forming units (CFU) assay[12]. We furthermore used the specific primers[12] for *C. testosteroni*, *C. meningosepticum* and *S. marcescens*, which are found to be ones of most abundant cultivable bacteria species in the *A. aegypti* midgut[12], to ensure the removal by antibiotic treatment. After the antibiotic treatment, the mosquitoes were fed a mixture containing either *C. testosteroni* or *C.*

meningosepticum with fresh mouse blood (1:1 v/v) via the Hemotek® feeding system (6W1, Hemotek Limited, England). All supplies used in the mosquito feeding experiment (feeders, membrane, tips, etc.) were aseptic. The bacteria-fed mosquitoes were sacrificed for the gut isolation at several hours after blood feeding. Because of the short time interval, the mosquitoes will not receive a new portion of food that may introduce bacterial contamination.

Counting the oral-introduced bacterial number per insect gut

To determine the number of acquired bacteria in the gut of individual insect, a serial numbers of bacteria was exploited to feed the antibiotic-treated mosquitoes or germ-free flies. Twelve fed insects in each group were randomly selected for the gut isolation under aseptic conditions, and were ground in sterile PBS. The lysates of different dilutions were applied on LB plates without antibiotics. After overnight culture at 37°C, the number of bacteria on the plate was counted to calculate the number of acquired bacteria by per insect. For acquired bacteria counting in the mosquito midguts, a serial number of either *C. testosteroni* or *C. meningosepticum* (0.5 OD, 5 OD and 50 OD) were exploited to feed the antibiotic-treated mosquitoes. Twelve fed mosquitoes in each group were randomly selected for the gut isolation, and subsequently we did a bacterial count using a CFU assay. The number of bacteria ingested by a mosquito was approximately 5.4×10^5 cells in 0.5 OD, 4.3×10^6 cells in 5 OD, and 3.7×10^7 cells in 50 OD *C. testosteroni*-fed mosquitoes, and 5.2×10^5 cells in 0.5 OD, 8.3×10^6 cells in 5 OD, and 9.6×10^7 cells in 50 OD *C. meningosepticum*-fed mosquitoes (Supplementary Fig. 18a,b). For bacteria counting in the fly guts, a serial amounts of *A. thailandicus* (1 OD, 50 OD and 250 OD), gradually mixed with the standard *Drosophila* food respectively, was exploited to feed the germ-free flies. Twelve fed flies in each group were randomly selected to isolate the guts for bacterial counting. The quantity of bacteria ingested by a fly was approximately 4.4×10^4 cells in 1 OD, 6.0×10^6 cells in 50 OD, and 4.9×10^8 cells in 250 OD bacteria-fed flies (Supplementary Fig. 18c).

Bacterial isolation from the insect guts

The insect surface was sterilized with 70% ethanol and washed twice with sterile PBS. The guts of mosquitoes or flies were carefully removed from the abdomen into PBS buffer, and ground adequately under aseptic conditions to reduce contamination from surrounding bacteria. The gut lysates were plated on LB plate without antibiotics, and cultured at 37°C. We identified *C. testosteroni, C. meningosepticum* from *Aedes aegypti,* and *A. thailandicus* from *Drosophila melanogaster*.

Measurement of gut microbiome by 16S rRNA qPCR

The total RNA of the guts was extracted from the sample with the RNeasy Mini Kit (Qiagen, Cat. No# 74106). cDNA was randomly reverse-transcribed by an iScript cDNA Synthesis Kit (Bio-Rad, Cat. No# 1708891). A commercial matrix was used for qPCR assay (Bio-Rad Cat. No#172-5121). The 16S rRNA was amplified using universal primers[27] and bacterial specific primers[12]. The burden of the gut microbiome was normalized to *A. aegypti actin* (*AAEL011197*) or *D. melanogaster actin* (*CG12051*).

H_2O_2 assay for determination of ROS activity

The insect guts were dissected in PBS with 2 mg/ml of the catalase inhibitor 3-amino-1,2,4-triazole (A8056-10G, Sigma) at different time points. After homogenization, the samples were filtered through a spin filter with a 10K molecular weight cutoff (Corning, Corning Spin-XUF, Cat. No# 431486). The eluate from each experimental group was then collected and tested using a hydrogen peroxide assay kit (BioVision, Cat. No# K265-200). The fluorescence intensity was measured at an excitation wavelength of 550 nm and an emission wavelength of 590 nm using a fluorescence microplate reader according to the manufacturer's instructions.

Dihydroethidium staining

The mosquito midguts were dissected in PBS containing the catalase inhibitor 3-amino-1,2,4-triazole (A8056, Sigma). Immediately after dissection, the midguts were incubated with 2 μM dihydroethidium (DHE) (D7008, Sigma) in PBS at RT for 30 min in the dark. Then, the midguts were fixed with 4% PFA for 30 min and incubated for an additional 30 min with Triton X-100. Nuclei were stained blue with To-Pro-3 iodide (Thermo-Fisher Scientific, Cat. No# T3605). Slides were imaged using a 10×objective lens on a Zeiss LSM 780 meta confocal microscope (Carl Zeiss, Germany) in a multi-track mode.

Smurf assay

The dyes Blue dye no. 1 or Red dye no. 40 purchased from Sigma-Aldrich (2.5% wt/vol) were premixed with *Drosophila* standard food respectively. Flies were reared on the medium with dyes for 12 hours. The dissemination of dyes were subsequently recorded in the fed *Drosophila* bodies.

RNA-Seq analysis of mosquito midguts

Total RNA was extracted with TRIzol (Ambion Cat. No# 15596018) from pools of 60 midguts of the *AaMesh* dsRNA-inoculated (Day 3 and Day 6) and AaMesh antiserum-fed (18 hours) female *A. aegypti* mosquitoes. The samples were delivered to the Beijing Genomics Institute (Shenzhen, China) for commercial RNA-Seq services and data analysis. Clean reads were mapped to the *A. aegypti* transcript database using SOAPaligner/SOAP2 mismatches. The number of clean reads for each gene was calculated and then normalized to Reads per Kb per Million reads (RPKM), which associates read numbers with gene expression levels. The $\log_2$ ratio (read number in AaMesh-suppressed midgut/read number in control midgut) was exploited to determine gene regulation. Immune genes with $\log_2$ ratio ≤ -0.4 were selected for further analysis[38,48]. A rigorous algorithm was used to screen for differentially expressed genes in each group. The sequencing data were deposited in the Short Read Archive (NCBI) with accession number GSE79070.

Statistics

Animals were randomly allocated into different groups. Mosquitoes and flies that died before measurement were excluded from analysis. The investigators were not blinded to the allocation during the experiments or to the outcome assessment. Descriptive statistics have

been provided in the figure legends. Given the nature of the experiments and the type of samples, differences in continuous variables were assessed with the non-parametric *Mann-Whitney* test. All analyses were performed using GraphPad Prism statistical software.

Data availability

The data that support the findings of this study are available from the corresponding author upon reasonable request. Please see methods for specific data sets.

Supplementary Material

Refer to Web version on PubMed Central for supplementary material.

Acknowledgments

This work was funded by the grants from the National Key Research and Development Plan of China (2016YFD0500400, 2016YFC1201000, 2016ZX10004001-008), the grants from the National Natural Science Foundation of China (81422028, 81571975, 61472205, 31171278, and 31271542), and the grant from National Institute of Health of the United States (AI103807). We thank Professor Won-Jae Lee from Seoul National University to provide *Erwinia carotovora carotovora 15* for the study. We thank that Professor George K. Christophides from Imperial College London provided critical suggestions for this manuscript. G.C. is a Newton Advanced Fellow awarded by the Academy of Medical Sciences and the Newton Fund, and a Janssen Investigator of Tsinghua University. We thank the technical supports from the Core Facility of Center for Life Sciences and Center of Biomedical Analysis (Tsinghua University).

References

1. Koropatnick TA, et al. Microbial factor-mediated development in a host-bacterial mutualism. Science. 2004; 306:1186–1188. [PubMed: 15539604]
2. Macdonald TT, Monteleone G. Immunity, inflammation, and allergy in the gut. Science. 2005; 307:1920–1925. [PubMed: 15790845]
3. Backhed F, Ley RE, Sonnenburg JL, Peterson DA, Gordon JI. Host-bacterial mutualism in the human intestine. Science. 2005; 307:1915–1920. [PubMed: 15790844]
4. Clark RI, et al. Distinct shifts in microbiota composition during *Drosophila* aging impair intestinal function and drive mortality. Cell Rep. 2015; 12:1656–1667. [PubMed: 26321641]
5. Artis D. Epithelial-cell recognition of commensal bacteria and maintenance of immune homeostasis in the gut. Nat Rev Immunol. 2008; 8:411–420. [PubMed: 18469830]
6. Ha EM, et al. Regulation of DUOX by the Galphaq-phospholipase C beta-Ca^{2+} pathway in *Drosophila* gut immunity. Dev Cell. 2009a; 16:386–397. [PubMed: 19289084]
7. Ha EM, et al. Coordination of multiple dual oxidase-regulatory pathways in responses to commensal and infectious microbes in *Drosophila* gut. Nat Immunol. 2009b; 10:949–957. [PubMed: 19668222]
8. Lhocine N, et al. PIMS modulates immune tolerance by negatively regulating *Drosophila* innate immune signaling. Cell Host Microbe. 2008; 4:147–158. [PubMed: 18692774]
9. Paredes JC, Welchman DP, Poidevin M, Lemaitre B. Negative regulation by amidase PGRPs shapes the *Drosophila* antibacterial response and protects the fly from innocuous infection. Immunity. 2011; 35:770–779. [PubMed: 22118526]
10. Ryu JH, et al. Innate immune homeostasis by the homeobox gene *caudal* and commensal-gut mutualism in *Drosophila*. Science. 2008; 319:777–782. [PubMed: 18218863]
11. Cullen TW, et al. Gut microbiota. Antimicrobial peptide resistance mediates resilience of prominent gut commensals during inflammation. Science. 2015; 347:170–175. [PubMed: 25574022]
12. Pang XJ, et al. Mosquito C-type lectins maintain gut microbiome homeostasis. Nature microbiology. 2016 Article number: 16023.

13. Hegde S, Rasgon JL, Hughes GL. The microbiome modulates arbovirus transmission in mosquitoes. Curr Opin Virol. 2015; 15:97–102. [PubMed: 26363996]
14. Kanellopoulos J. Studying host-microbiota interactions in *Drosophila melanogaster*. Biomed J. 2015; 38:275. [PubMed: 26265546]
15. Oliveira JH, et al. Blood meal-derived heme decreases ROS levels in the midgut of *Aedes aegypti* and allows proliferation of intestinal microbiota. PLoS Pathog. 2011; 7:e1001320. [PubMed: 21445237]
16. Yao Z, et al. The dual oxidase gene BdDuox regulates the intestinal bacterial community homeostasis of *Bactrocera dorsalis*. ISME J. 2015; 10:1037–1050. [PubMed: 26565723]
17. Diaz-Albiter H, Sant'Anna MR, Genta FA, Dillon RJ. Reactive oxygen species-mediated immunity against *Leishmania mexicana* and *Serratia marcescens* in the sand phlebotomine fly *Lutzomyia longipalpis*. J Biol Chem. 2012; 287:23995–24003. [PubMed: 22645126]
18. Bae YS, Choi MK, Lee WJ. Dual oxidase in mucosal immunity and host-microbe homeostasis. Trends Immunol. 2010; 31:278–287. [PubMed: 20579935]
19. Waterhouse RM, et al. Evolutionary dynamics of immune-related genes and pathways in disease-vector mosquitoes. Science. 2007; 316:1738–1743. [PubMed: 17588928]
20. Dempsey PW, Allison ME, Akkaraju S, Goodnow CC, Fearon DT. C3d of complement as a molecular adjuvant: bridging innate and acquired immunity. Science. 1996; 271:348–350. [PubMed: 8553069]
21. Casasnovas JM, Larvie M, Stehle T. Crystal structure of two CD46 domains reveals an extended measles virus-binding surface. EMBO J. 1999; 18:2911–2922. [PubMed: 10357804]
22. Dörig RE, Marcil A, Chopra A, Richardson CD. The human CD46 molecule is a receptor for measles virus (Edmonston strain). Cell. 1993; 75:295–305. [PubMed: 8402913]
23. Xiao X, et al. Complement-related proteins control the flavivirus infection of *Aedes aegypti* by inducing antimicrobial peptides. PLoS Pathog. 2014; 10:e1004027. [PubMed: 24722701]
24. Xiao X, et al. A neuron-specific antiviral mechanism prevents lethal flaviviral infection of mosquitoes. PLoS Pathog. 2015; 11:e1004848. [PubMed: 25915054]
25. Izumi Y, Yanagihashi Y, Furuse M. A novel protein complex, Mesh-Ssk, is required for septate junction formation in the *Drosophila* midgut. J Cell Sci. 2012; 125:4923–4933. [PubMed: 22854041]
26. Rämet M, et al. *Drosophila* scavenger receptor CI is a pattern recognition receptor for bacteria. Immunity. 2001; 15:1027–1038. [PubMed: 11754822]
27. Kumar S, Molina-Cruz A, Gupta L, Rodrigues J, Barillas-Mury C. A peroxidase/dual oxidase system modulates midgut epithelial immunity in *Anopheles gambiae*. Science. 2010; 327:1644–1648. [PubMed: 20223948]
28. Chintapalli VR, Wang J, Dow JA. Using FlyAtlas to identify better *Drosophila melanogaster* models of human disease. Nat Genet. 2007; 39:715–720. [PubMed: 17534367]
29. Robinson SW, Herzyk P, Dow JA, Leader DP. FlyAtlas: database of gene expression in the tissues of *Drosophila melanogaster*. Nucleic Acids Res. 2013; 41:D744–750. [PubMed: 23203866]
30. Rera M, Clark RI, Walker DW. Intestinal barrier dysfunction links metabolic and inflammatory markers of aging to death in *Drosophila*. Proc Natl Acad Sci U S A. 2012; 109:21528–21533. [PubMed: 23236133]
31. Jones RM, et al. Symbiotic *lactobacilli* stimulate gut epithelial proliferation via Nox-mediated generation of reactive oxygen species. Embo J. 2013; 32:3017–3028. [PubMed: 24141879]
32. Chakrabarti S, Poidevin M, Lemaitre B. The *Drosophila* MAPK p38c regulates oxidative stress and lipid homeostasis in the intestine. PLoS Genet. 2014; 10:e1004659. [PubMed: 25254641]
33. DeWire SM, Ahn S, Lefkowitz RJ, Shenoy SK. Beta-arrestins and cell signaling. Annu Rev Physiol. 2007; 69:483–510. [PubMed: 17305471]
34. Ramirez JL, et al. Reciprocal tripartite interactions between the *Aedes aegypti* midgut microbiota, innate immune system and dengue virus influences vector competence. PLoS Negl Trop Dis. 2012; 6:e1561. [PubMed: 22413032]
35. Nittaya Pitiwittayakul PY, Winai Chaipitakchonlatarn YY, Theeragool G. *Acetobacter thailandicus* sp. nov., for a strain isolated in Thailand. Ann Microbiol. 2015; 65:1855–1863.

36. Chaston JM, Newell PD, Douglas AE. Metagenome-wide association of microbial determinants of host phenotype in *Drosophila melanogaster*. MBio. 2014; 5:e01631. [PubMed: 25271286]
37. Sommer F, Backhed F. The gut microbiota engages different signaling pathways to induce Duox2 expression in the ileum and colon epithelium. Mucosal Immunol. 2015; 8:372–379. [PubMed: 25160818]
38. Lee KA, et al. Bacterial-derived uracil as a modulator of mucosal immunity and gut-microbe homeostasis in *Drosophila*. Cell. 2013; 153:797–811. [PubMed: 23663779]
39. Wang WX, et al. Molecular and functional characterization of a c-type lysozyme from the Asian corn borer, *Ostrinia furnacalis*. J Insect Sci. 2009; 9:17–29. [PubMed: 19613460]
40. Yu LP, Sun BG, Li J, Sun L. Characterization of a c-type lysozyme of Scophthalmus maximus: expression, activity, and antibacterial effect. Fish Shellfish Immunol. 2013; 34:46–54. [PubMed: 23063540]
41. Gravato-Nobre MJ, Vaz F, Filipe S, Chalmers R, Hodgkin J. The invertebrate lysozyme effector ILYS-3 is systemically activated in response to danger signals and confers antimicrobial protection in *C. elegans*. PLoS Pathog. 2016; 12:e1005826. [PubMed: 27525822]
42. Liu Y, et al. Transmission-blocking antibodies against mosquito C-type lectins for dengue prevention. PLoS Pathog. 2014; 10:e1003931. [PubMed: 24550728]
43. Cheng G, et al. A C-type lectin collaborates with a CD45 phosphatase homolog to facilitate West Nile virus infection of mosquitoes. Cell. 2010; 142:714–725. [PubMed: 20797779]
44. Yu Z, et al. Highly efficient genome modifications mediated by CRISPR/Cas9 in *Drosophila*. Genetics. 2013; 195:289–291. [PubMed: 23833182]
45. Kim HJ, Lee HJ, Kim H, Cho SW, Kim JS. Targeted genome editing in human cells with zinc finger nucleases constructed via modular assembly. Genome Res. 2009; 19:1279–1288. [PubMed: 19470664]
46. Ni JQ, et al. A genome-scale shRNA resource for transgenic RNAi in *Drosophila*. Nat Methods. 2011; 8:405–407. [PubMed: 21460824]
47. Xi Z, Ramirez JL, Dimopoulos G. The *Aedes aegypti* toll pathway controls dengue virus infection. PLoS Pathog. 2008; 4:e1000098. [PubMed: 18604274]
48. Huang Y, Ng FS, Jackson FR. Comparison of larval and adult *Drosophila* astrocytes reveals stage-specific gene expression profiles. G3 (Bethesda). 2015; 5:551–558. [PubMed: 25653313]

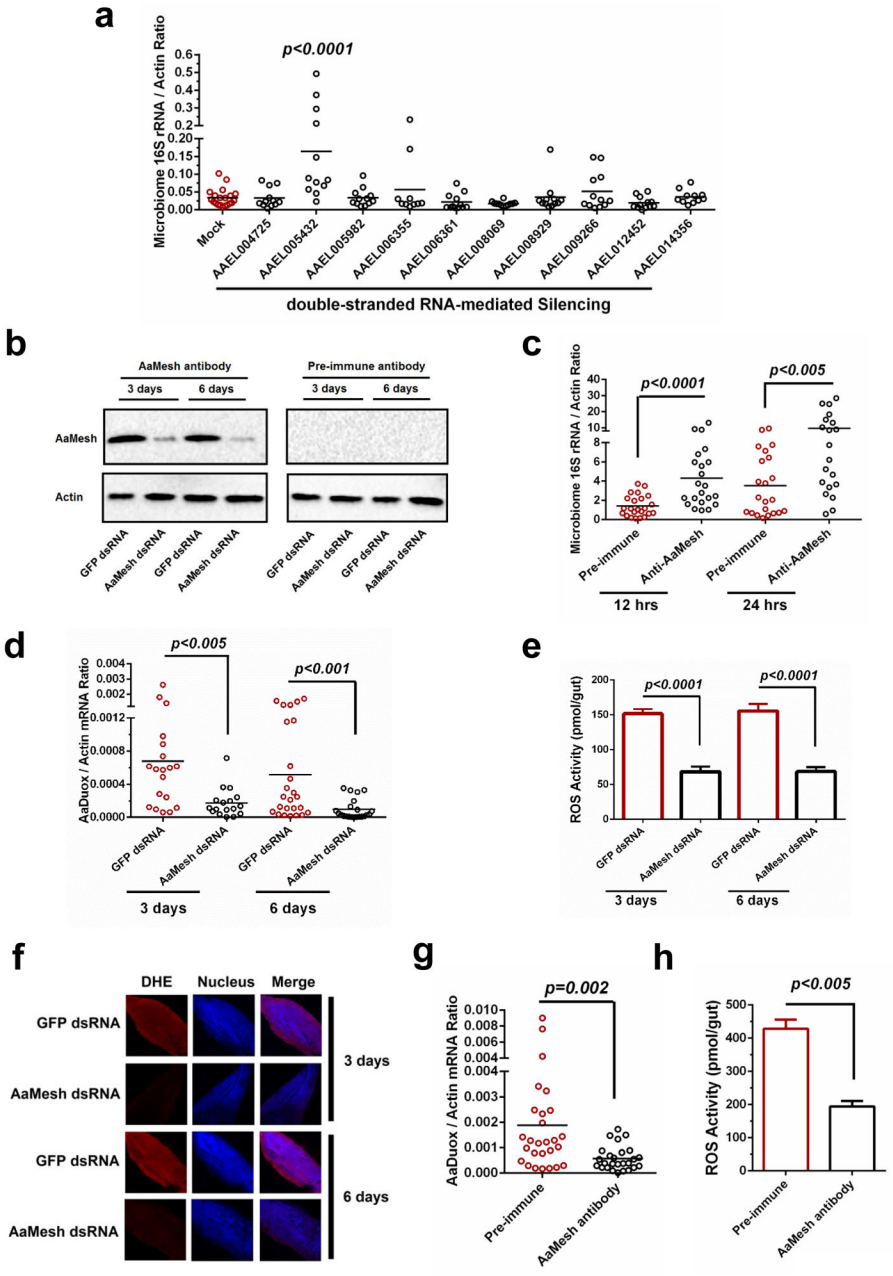

Figure 1. Mesh maintains gut microbiome homeostasis by controlling *AaDuox* expression in *A. aegypti*

(a) The roles of the *CCP* genes in the maintenance of the gut microbiome in *A. aegypti*. The genes were individually silenced via thoracic microinjection of dsRNA. The results were combined from 2 independent experiments.

(b) Validation of an AaMesh antibody in the guts of *AaMesh*-silenced mosquitoes. The amount of AaMesh was assessed via immuno-blotting with a murine AaMesh antibody in the mosquito lysates. Pre-immune serum served as a negative control. A total of 50 μg of protein from mosquito lysates was loaded into each lane.

(c) Immuno-blockade of AaMesh enhanced colonization of gut bacteria in the midgut of *A. aegypti*. The burden of the gut microbiome was detected by SYBR Green qPCR.
(d–f) Regulation of both *Duox* expression (d) and ROS activity (e and f) in the guts of *AaMesh* silencing mosquitoes. The *GFP* dsRNA-treated mosquitoes served as mock controls. ROS activity was measured by H_2O_2 assay (e) and Dihydroethidium staining (DHE) (f). (f) Nuclei were stained blue with To-Pro-3 iodide. Images were examined using a 10×objective lens on a Zeiss LSM 780 meta confocal microscope.
(g–h) Immuno-blockade of AaMesh impaired both *Duox* expression (g) and ROS activity (h) in the mosquito guts. The midguts of were collected at 18 hours after a blood meal. ROS activity was detected by H_2O_2 assay.
(a, c, d, g) In the mosquito midguts, the gene expression was determined by SYBR Green qPCR and normalized against *A. aegypti actin* (*AAEL011197*). The qPCR primers are described in Supplementary Table 6. One dot represents one gut. The horizontal line represents the mean value of the results.
(c, g, h) The murine AaMesh antibody, in a 100-fold serial dilution, was premixed with fresh mouse blood for the mosquito blood meal. Pre-immune serum at the same dilution served as a negative control.
(e, h) The data are presented as the mean ± S.E.M.
(a, c, d, e, g, h) The data were analyzed using the non-parametric *Mann-Whitney* test.
(b–h) All results were repeated in at least 3 independent experiments.

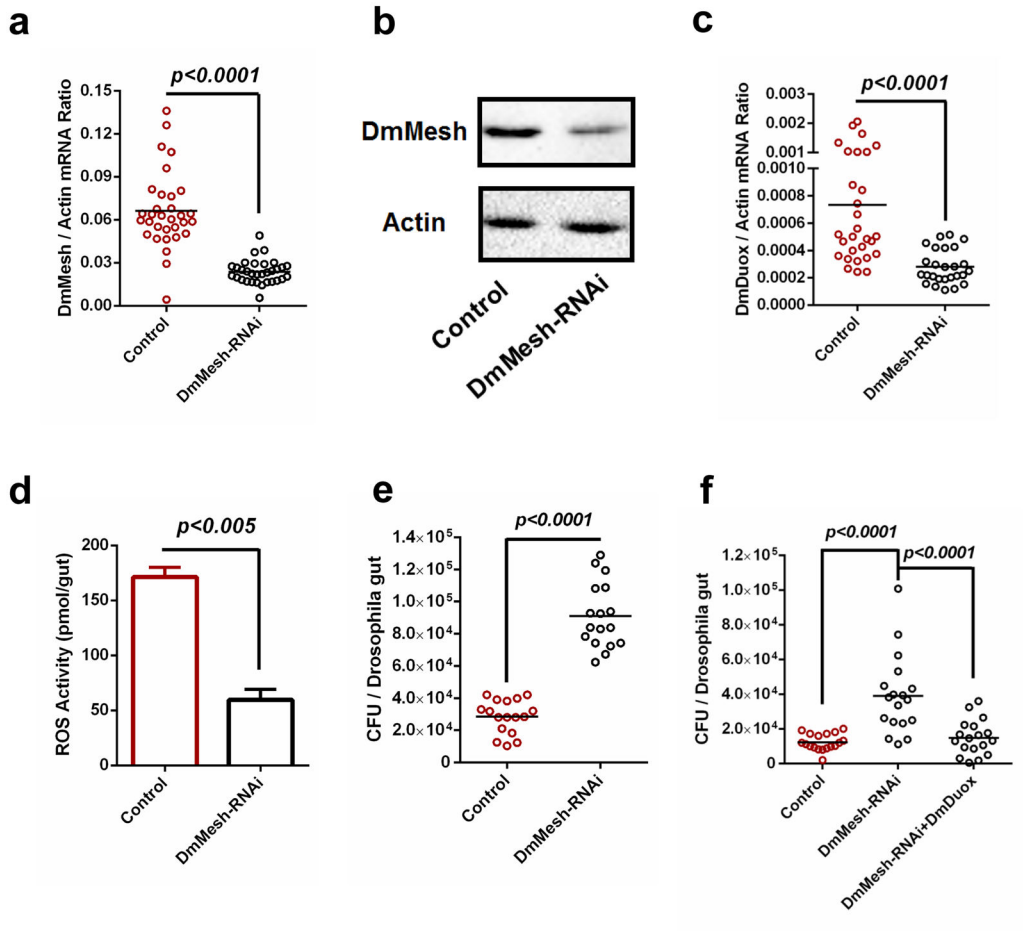

Figure 2. Regulation of commensal microbiome and *DmDuox* expression in the guts of *DmMesh* RNAi *Drosophila*

(a–b) Knockdown efficiency of *DmMesh* gene in the guts of *DmMesh* RNAi *Drosophila*. The *DmMesh* RNAi *Drosophila* strain was generated using a *GAL4* line driven by a midgut-specific *NP3084* promoter. The *NP3084/GFP-RNAi* flies served as a negative control. The knockdown efficiency in the guts of *DmMesh* RNAi flies was assessed via SYBR Green qPCR (a) and immuno-blotting with an AaMesh antibody (b). (b) A total of 50 μg of protein from mosquito lysates was loaded into each lane.

(c–d) Regulation of the *DmDuox* gene (c) and ROS activity (d) in the guts of *DmMesh* RNAi *Drosophila*. (d) ROS activity was measured by H_2O_2 assay. The data are presented as the mean ± S.E.M.

(e) Regulation of the gut microbiome in the guts of *DmMesh* RNAi *Drosophila*. The burden of the gut microbiome was determined by a colony-forming unit (CFU) assay.

(f) Reduction of burden of gut microbiome by rescuing *DmDuox* into the *DmMesh* RNAi flies. The burden of the gut microbiome was determined by a CFU assay.

(a, c) The gene expression was determined by SYBR Green qPCR and normalized against *D. melanogaster* actin (*CG12051*). The qPCR primers are described in Supplementary Table 6. One dot represents one fly gut. The horizontal line represents the mean value of the results.

(a–f) All results were repeated in at least 3 independent experiments.

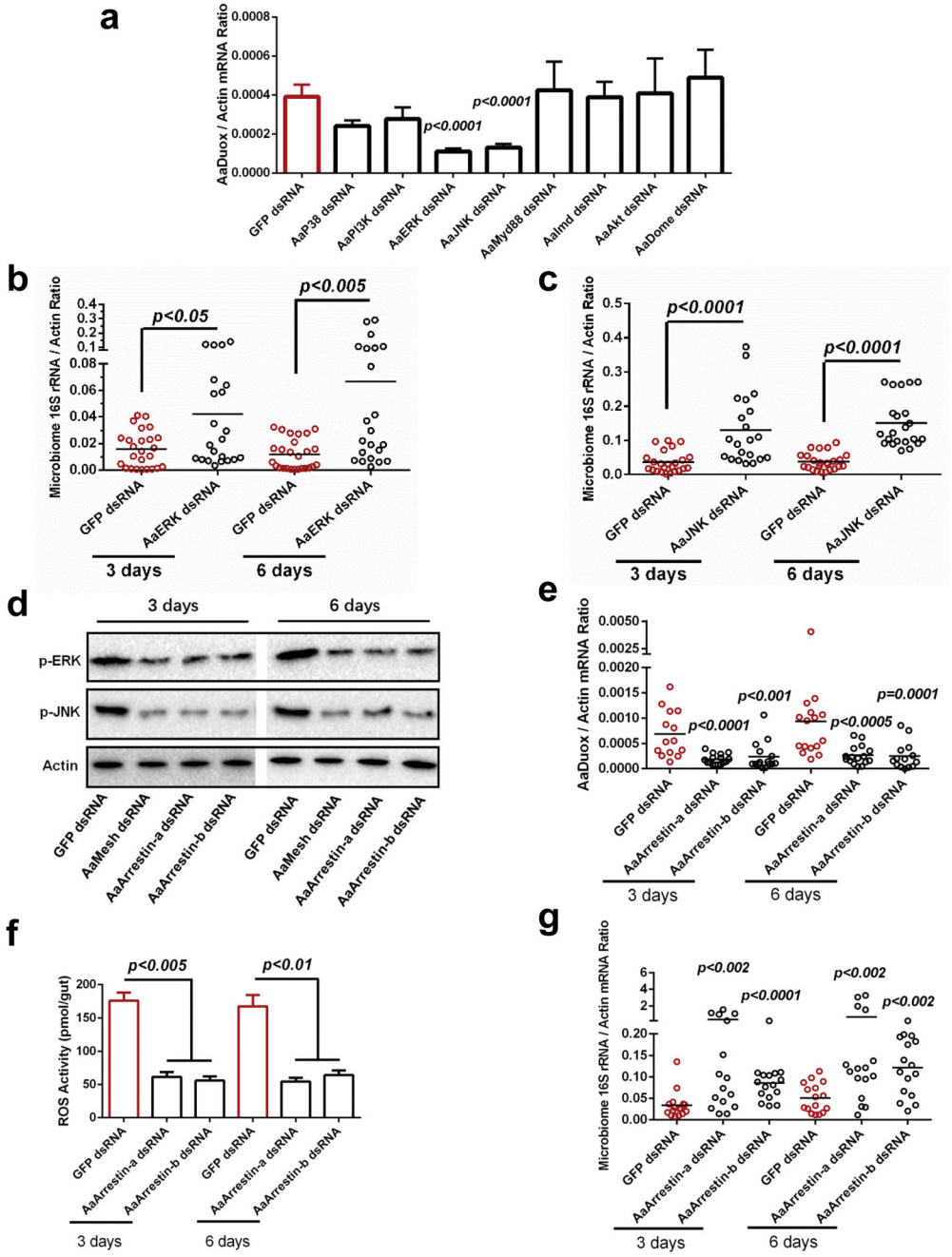

Figure 3. Mesh regulates *AaDuox* expression via Arrestin-mediated MAPK phosphorylation in *A. aegypti*

(a) The role of immune signaling pathways in regulating *Duox* expression in the midgut of *A. aegypti*. The genes of immune signaling components were knocked down by dsRNA thoracic inoculation. Six days later, the abundance of the *Duox* gene was determined in the midgut of *A. aegypti* by SYBR Green qPCR.

(b–c) Knockdown of *AaERK* and *AaJNK* enhanced the burden of the gut microbiome in *A. aegypti*. Both *AaERK* and *AaJNK* were silenced by dsRNA thoracic inoculation in *A.*

aegypti. The midguts were isolated 3 and 6 days after gene silencing, and the burden of the gut microbiome was subsequently determined by SYBR Green qPCR.
(d) Genetic suppression of *AaMesh* and *AaArrestins* impaired the phosphorylation of AaERK and AaJNK in the mosquito guts. *AaMesh* and *AaArrestins* were silenced by dsRNA thoracic inoculation in *A. aegypti*, respectively. The midguts were isolated 3 and 6 days after gene silencing, and the phosphorylation of AaERK (p-ERK) and AaJNK (p-JNK) were subsequently determined by western blotting. A total of 50 μg of protein from mosquito gut lysates was loaded into each lane.
(e–f) Reduction of *Duox* expression (e) and ROS activity (f) in the guts of *AaArrestins*-silenced mosquitoes. The midguts from the dsRNA-treated mosquitoes were isolated for the detection of *Duox* expression (e) by SYBR Green qPCR and for measuring ROS activity using a H_2O_2 assay (f). (f) The data are presented as the mean ± S.E.M.
(g) Silencing *AaArrestins* increased the load of the gut microbiome in *A. aegypti*.
(a, b, c, e, g) The *GFP* dsRNA-treated mosquitoes served as mock controls. The gene expression was determined by SYBR Green qPCR and normalized against *A. aegypti actin* (*AAEL011197*). The qPCR primers are described in Supplementary Table 6. One dot represents one gut. The horizontal line represents the mean value of the results.
(a, f) The data are presented as the mean ± S.E.M.
(a–c, e–g) The data were analyzed using the non-parametric *Mann-Whitney* test.
(a–g) All results were repeated in at least 3 independent experiments.

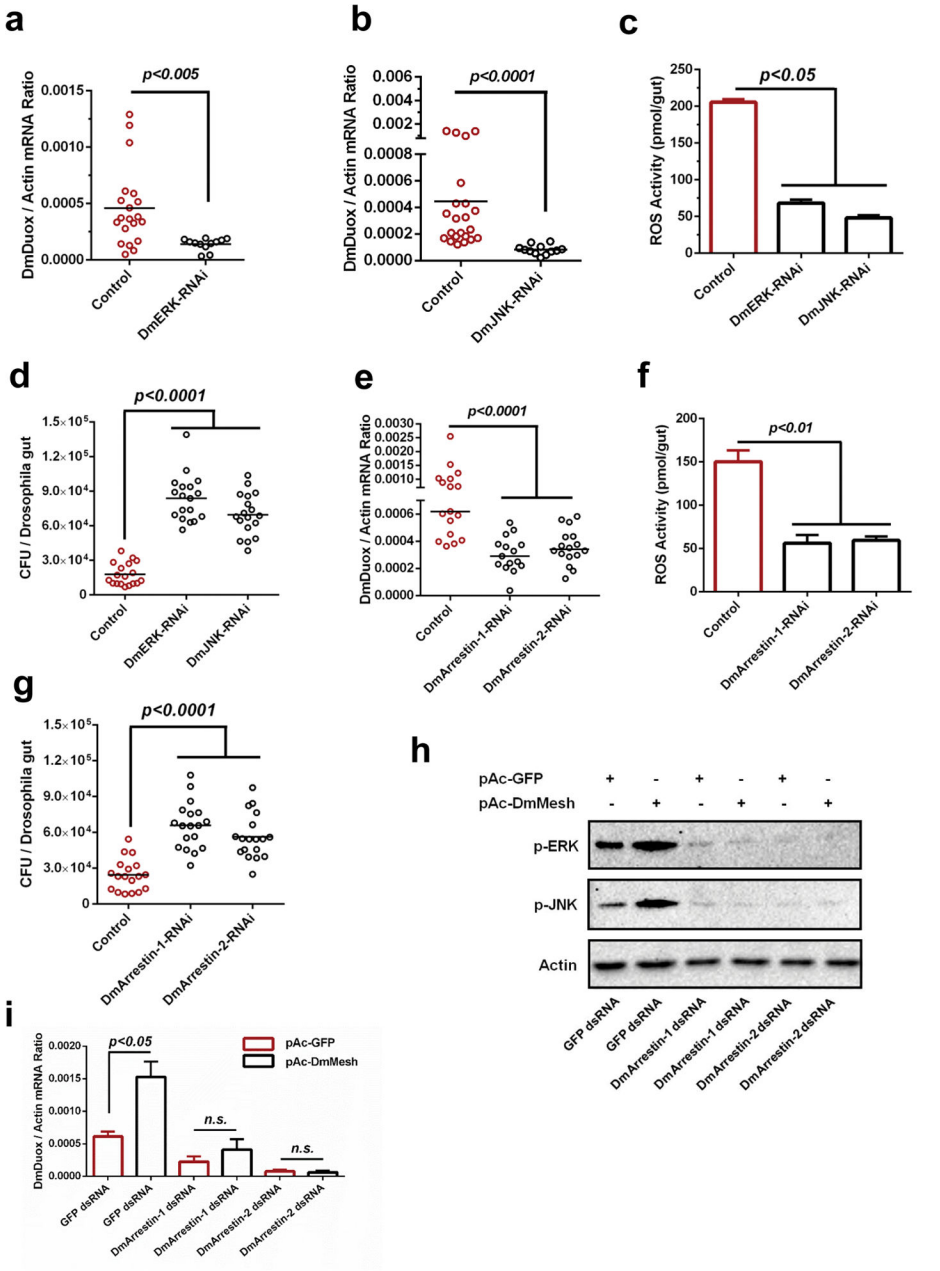

Figure 4. The role of Mesh-Arrestin-ERK/JNK-MAPK signaling cascade in *DmDuox* regulation in *Drosophila*

(a–b) Regulation of the *DmDuox* gene in the guts of *DmERK* (a) and *DmJNK* (b) RNAi flies.

(c) Regulation of ROS activity in the guts of *DmERK* and *DmJNK* RNAi flies.

(d) Enhancement of the gut microbiome in the guts of *DmERK* and *DmJNK* RNAi flies.

(e–f) Silencing *DmArrestins* impaired expression of the *DmDuox* gene (e) and ROS activity (f) in the *Drosophila* guts.

(g) Increasing the burden of gut microbiome in the guts of *DmArrestins* RNAi flies.

(h–i) Assessing the role of the "Arrestin-ERK/JNK" cascade in AaMesh-mediated *Duox* expression in *Drosophila*. Both *DmArrestin-1* and *DmArrestin-2* were silenced by dsRNA transfection in the pAc-DmMesh-trnasfected *Drosophila* S2 cells. (h) The phosphorylation of DmERK (p-ERK) and DmJNK (p-JNK) was detected by western blotting. (i) The abundance of the *DmDuox* gene was determined by SYBR Green qPCR and normalized by *Drosophila actin* (*CG12051*).

(a–g) *GFP* RNAi flies served as a negative control.

(a–b, e) The gene expression was determined by SYBR Green qPCR and normalized against *D. melanogaster actin* (*CG12051*). The qPCR primers are described in Supplementary Table 6. One dot represents one fly gut. The horizontal line represents the mean value of the results.

(c, f) The ROS activity was detected by a H_2O_2 assay. The data are presented as the mean ± S.E.M.

(d, g) The burden of gut microbes was determined by a CFU assay.

(a–g, i) The data were analyzed using the non-parametric *Mann-Whitney* test.

(a–i) The results were reproduced by at least 3 independent experiments.

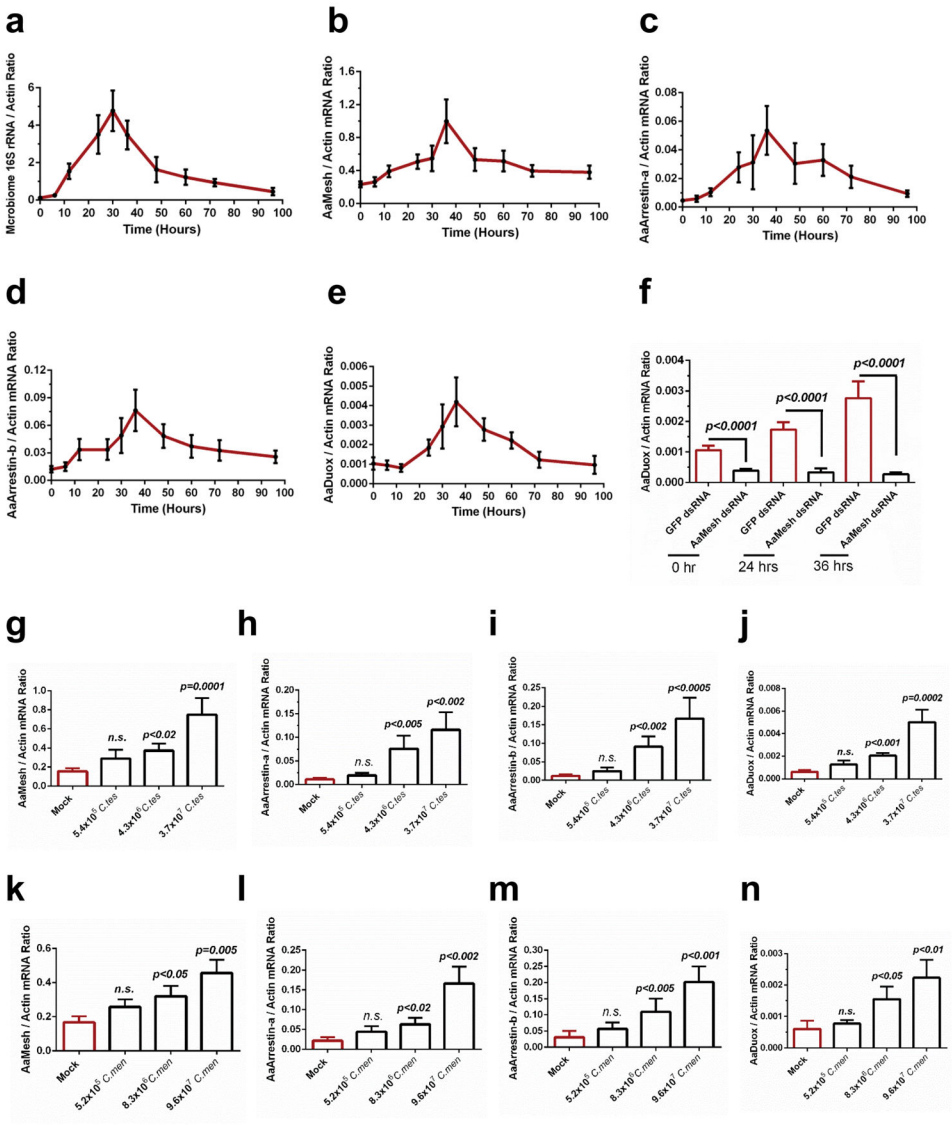

Figure 5. The AaMesh-mediated *AaDuox* regulatory pathway in response to commensal bacteria in the guts of *A. aegypti*

Responses of the AaMesh-mediated *AaDuox* regulatory pathway to the blood meal-mediated augmentation of gut commensal bacteria (a–f), and oral introduction of the commensal microbiome *C. testosteroni* (*C. tes*, g–j) and *C. meningosepticum* (*C. men*, k–n), in the gut of *A. aegypti*.

(a) Regulation of the gut microbiome after a blood meal in the mosquito guts.

(b–e, g–n) Regulation of the *AaMesh* (b, g, k), *AaArrestin-a* (c, h, l), *AaArrestin-b* (d, i, m) and *AaDuox* (e, j, n) genes in the mosquito midguts.

(f) Silencing *AaMesh* abolished the induction of the *AaDuox* gene after a blood meal.

(g–n) These bacteria were introduced into the guts of antibiotic-treated mosquitoes. Measurement of the average bacterial number introduced into each mosquito gut was presented by Supplementary Fig. 18. The genes were determined at 12 hours post blood-mediated bacterial introduction.

(a–n) Both the burden of the gut microbes and the gene abundance were determined by SYBR Green qPCR and normalized against *A. aegypti actin* (*AAEL011197*). The qPCR primers are described in Supplementary Table 6. The data are presented as the mean ± S.E.M. All results were repeated by 3 independent experiments. The data were analyzed using the non-parametric *Mann-Whitney* test.

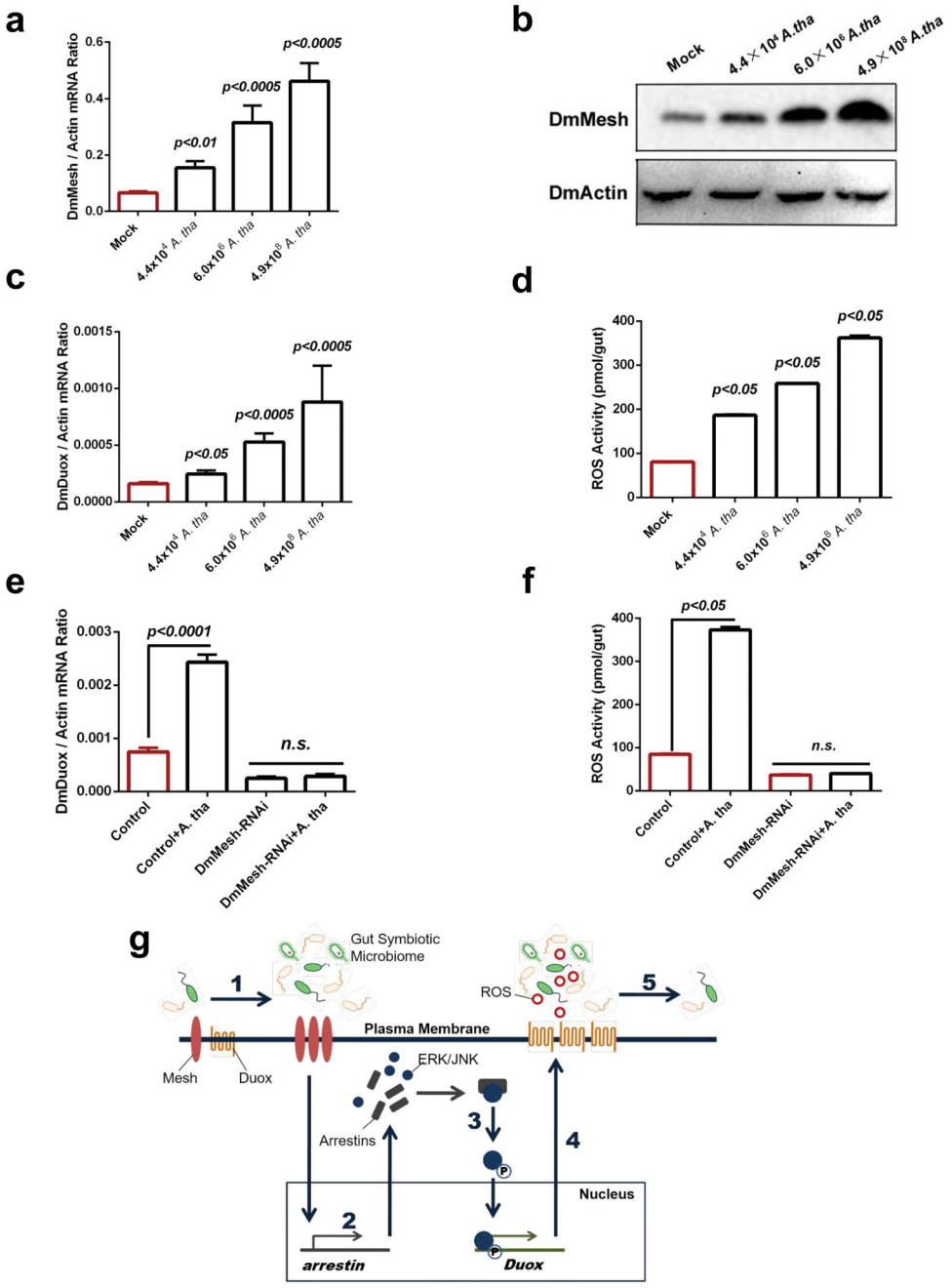

Figure 6. The DmMesh-mediated *DmDuox* regulation in response to commensal bacteria in *Drosophila*

(a–d) Oral introduction of *A. thailandicus* (*A. tha*) induced the *DmMesh* expression and DmDuox-mediated ROS in the gut of aseptic *Drosophila*. *A. thailandicus* was orally introduced into the germ-free *DmMesh* RNAi flies by food ingestion. Measurement of the average bacterial number introduced into each fly gut was presented by Supplementary Figure 18. The mRNA expression levels of *DmMesh* (a) and *DmDuox* (c) were determined by SYBR Green qPCR. (b) The protein level of DmMesh was determined by Western-blot

with an anti-AaMesh murine antibody. (d) Detection of the ROS activity in the *Drosophila* midguts.

(e–f) The DmMesh-mediated *DmDuox* regulatory pathway in response to *A. thailandicus*. The *DmMesh* RNAi *Drosophila* strain was generated using a *GAL4* line driven by a *NP3084* promoter. The germ-free *NP3084/GFP-RNAi* flies that fed on the same bacteria served as negative controls. 6×10^6 *A. thailandicus* was orally introduced into the germ-free *DmMesh* RNAi flies by food ingestion. (e) Measurement of *DmDuox* expression and (f) the ROS activity in the *Drosophila* midguts.

(g) Schematic representation of the AaMesh-mediated *Duox* regulatory pathway in response to symbiotic gut microbes. The expression of *Mesh* can be upregulated by the proliferation of the symbiotic microbiome in insect guts (1). Because Mesh is a positive regulator of *Arrestin* expression, induction of Mesh results in a higher abundance of Arrestins (2), and subsequently accelerates the phosphorylation of the ERK and JNK MAPK proteins (3). The activation of ERK and JNK leads to the downstream *Duox* transcription (4). Thus, higher DUOX-mediated ROS are generated in response to the gut microbial proliferation, thereby moderating the proliferation of symbiotic microbes in gut-microbe homeostasis (5).

(a, c, e) The *Duox* expression was assessed by SYBR Green qPCR and normalized against *Drosophila actin*. The qPCR primers are described in Supplementary Table 6.

(d, f) The ROS activity was detected by a H_2O_2 assay.

(a, c–f) The data are presented as the mean ± S.E.M. All results were repeated by 3 independent experiments. The data were analyzed using the non-parametric *Mann-Whitney* test.